Measurement of emittance with the MICE scintillating fibre trackers

F. Drielsma on behalf of the MICE collaboration
Department of Nuclear and Particle Physics, University of Geneva,
24 Quai Ernest-Ansermet, CH-1211 Geneva, Switzerland

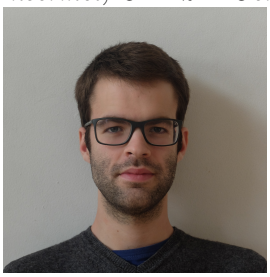

The Muon Ionization Cooling Experiment (MICE) collaboration will demonstrate the feasibility of ionization cooling, the technique by which it is proposed to cool the muon beam at a future neutrino factory or muon collider. The muon beam emittance is measured on a particle-by-particle basis. Measurements are made before and after the cooling cell using a high precision scintillating-fibre tracker in a solenoid magnetic field. A pure muon sample is selected using a particle identification system that can reject pions and electrons efficiently. The emittance of the MICE Muon Beam has been measured for the first time with the scintillating-fibre tracking system using the October 2015 commissioning data. The performance of the tracking and the analysis techniques required for this precision measurement are shown. The two spectrometers were powered together with the focus coil module in July 2016 and muon tracks were measured up and downstream of the cooling cell. The expected emittance change to be observed for a specific lattice in the ongoing MICE Step IV is summarized.

1 Introduction

Intense muon sources are required for a future Neutrino Factory or Muon Collider [1,2]. At production, muons occupy a large phase-space volume (emittance), which makes them difficult to accelerate and store. Therefore, the emittance of the muon beams must be reduced, i.e the muons must be "cooled", to maximise the muon flux delivered to the accelerator.

Conventional cooling techniques applied to muon beams [3] would leave almost no muons to be accelerated since the muon lifetime is short ($\tau_\mu \sim 2.2\,\mu$s). Almost a factor of a million in 6D muon cooling has been achieved in a simulation [4] which shows that the ionization-cooling effect builds quickly enough to deliver the flux and emittance required by the Neutrino Factory and the Muon Collider. The rate of change in normalised emittance when passing through an absorber can be approximated by the following "cooling equation"

$$\frac{d\varepsilon_N}{ds} \simeq -\frac{\varepsilon_N}{\beta^2 E_\mu}\left|\frac{dE_\mu}{ds}\right| + \frac{\beta_\perp\,(0.014)^2}{2\beta^3 E_\mu m_\mu X_0}\,. \tag{1}$$

The cooling equation shows that low-Z materials are preferred as they have a longer radiation length, X_0. The MICE collaboration will study the cooling equation in detail to demonstrate the feasibility of this technique [5]. It will investigate LiH and liquid H_2 absorbers as well as several input normalised emittance, ϵ_N, magnetic lattices, $\beta_\perp$, and muon energy, E_μ.

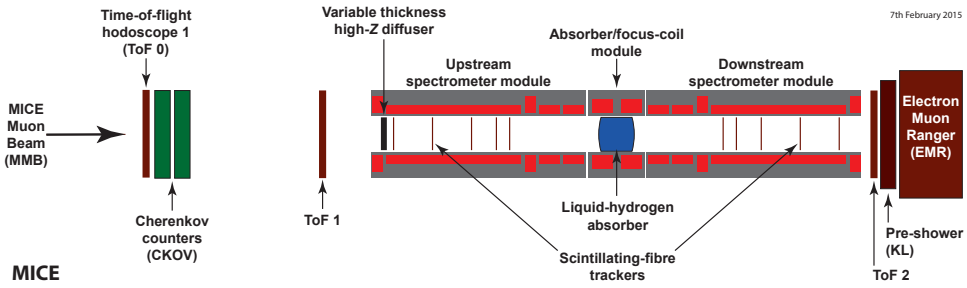

Figure 1 – Schematics of the MICE experiment at present. The muons produced in the MICE Muon Beam line first pass through the upstream particle identification (PID) apparatus, are sampled up and downstream of the absorber by scintillating fibre trackers before being dumped in the downstream PID section.

A schematic of the MICE experiment is shown in figure 1. The MICE Muon Beamline operates on the ISIS proton synchrotron at the Rutherford Appleton Laboratory. A titanium target [6] samples the ISIS proton beam. The muons, product of the pion decays, are momentum selected by a pair of dipoles and transported by two triplets of quadrupoles. The resultant beam is propagated through time-of-flight counters, TOF0 and TOF1, and Cherenkov detectors, Ckov, to the cooling cell. The variable-thickness brass and tungsten 'diffuser' allows tuning of the input emittance before the muons are measured in the upstream spectrometer solenoid using a scintillating-fibre tracker. The beam then passes through low-Z absorbers prior to being remeasured in the downstream tracker. Upon exiting the cooling cell the beam is incident upon the final time-of-flight detector, TOF2, a pre-shower detector, KL, and a fully active tracker-calorimeter, the Electron-Muon Ranger, EMR [7].

2 Single-particle measurement

MICE is a single-particle experiment. The emittance reduction is reconstructed by measuring the phase-space vector (x, y, p_x, p_y, p_z) of each individual muon before and after going through the absorber. Tracks are accumulated into a beam ensemble during the analysis process to measure the change in normalised emittance. The single-particle nature allows for global track matching throughout the experiment, i.e. the ability to associate a trace measured in the upstream tracker with one in the downstream tracker but also with the PID detectors. Figure 2 shows the a two dimensional projection of 25 simulated muon trajectories going through the MICE experiment.

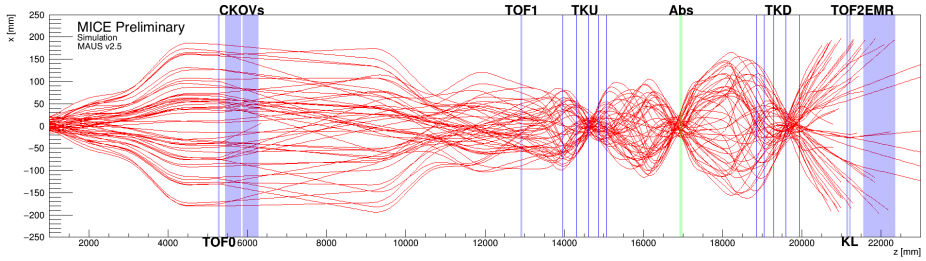

Figure 2 – Sample of 25 simulated virtual muon trajectories in the MICE. A tight focus, i.e. low $\beta_\perp$, can be clearly observed at the level of the absorber to minimize the heating term of the cooling equation.

Two identical scintillating-fibre trackers are symmetrically arranged about the absorber in uniform 4T fields. They each consist of five stations that sample the position of the muon track with $661 \pm 2\,\mu$m accuracy [8]. Particles were measured in the upstream tracking detector during a 4 T commissioning run in October 2015. The normalised transverse emittance of the set of accepted muons is reported in this paper.

3 Sample selection

The MICE Muon Beamline delivers a high purity beam with less than 1.4 % pion contamination [9]. The flight time between the first two time-of-flight hodoscopes (TOF0 and TOF1) is used to remove other contamination sources such as decay positrons from the final sample. In this measurement, muons with a flight time contained between 27 and 32 ns are accepted. The time-of-flight distribution of the final sample is shown in figure 3.

Provided with the position measurements in the five upstream tracker stations, a Kalman filter fits a single helical track to each muon trajectory, accounting for multiple scattering and energy loss in the scintillating material. The result provides the best estimate of the particle position and momentum in the station closest to the absorber [10] (reference plane).

The time-of-flight between TOF0 and TOF1 is represented as a function of the total momentum reconstructed in the tracker in figure 4. The dotted line represents the ideal time-of-flight of a muon that underwent the Bethe-Bloch most probable momentum loss between entering TOF1 and reaching the tracker reference plane.

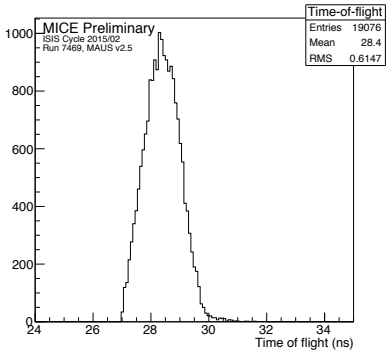

Figure 3 – Time-of-flight distribution between TOF0 and TOF1 of the final muon sample.

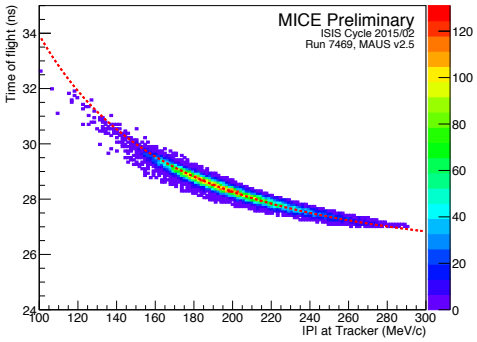

Figure 4 – Time-of-flight distribution between TOF0 and TOF1 as a function of the total momentum measured in the upstream tracker

4 Poincaré sections

In this analysis, a Poincaré section is a lower-dimensional subspace of the phase-space. The final sample of muons occupy a certain region of the phase-space of which two dimensional subspaces can be represented for simplicity. Figure 5 shows the $(x,\, y)$, $(x,\, p_x)$ and $(y,\, p_y)$ sections.

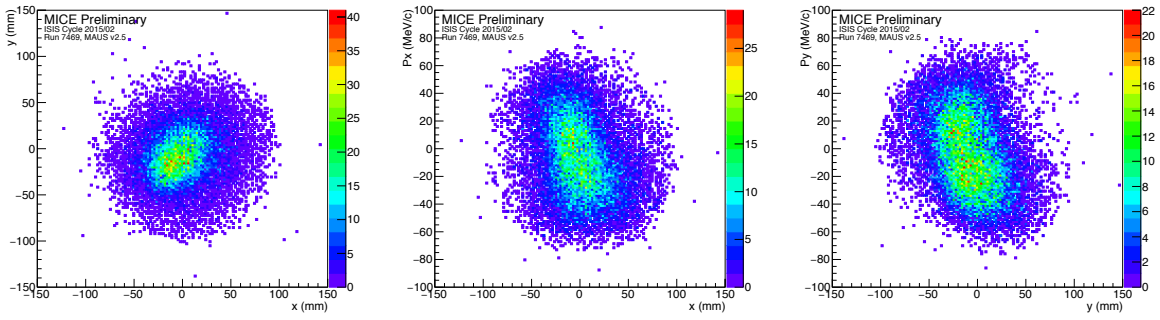

Figure 5 – Left to right: $(x,\, y)$, $(x,\, p_x)$ and $(y,\, p_y)$ Poincaré sections of the phase-space of muons.

Due to the large aperture dipoles used to momentum select the muon distribution, the selected muons sample contains dispersion in the horizontal plane. The sample shows a large

momentum spread, $\sigma_{p_z} \simeq 25.7\,\mathrm{MeV}/c$, for a mean longitudinal momentum, $\langle p_z \rangle = 195.4\,\mathrm{MeV}/c$. The emittance of the whole particle sample does not accurately represent the volume occupied by the particles the phase-space, as muons with different longitudinal momenta occupy different regions of the transverse phase-space. To remove the effect of the dispersion, the particle sample was pieced out in momentum-coherent $8\,\mathrm{MeV}/c$ bins.

5 Emittance

The transverse normalised emittance was calculated for each $8\,\mathrm{MeV}/c$ bin as

$$\epsilon_N = \frac{1}{m_\mu} \sqrt[4]{\det \Sigma}, \tag{2}$$

with m_μ the muon mass and Σ the 4D covariance matrix defined as

$$\Sigma = \begin{pmatrix} \sigma_{xx} & \sigma_{xy} & \sigma_{xp_x} & \sigma_{xp_y} \\ \sigma_{xy} & \sigma_{yy} & \sigma_{yp_x} & \sigma_{yp_y} \\ \sigma_{xp_x} & \sigma_{yp_x} & \sigma_{p_xp_x} & \sigma_{p_xp_y} \\ \sigma_{xp_y} & \sigma_{yp_y} & \sigma_{p_xp_y} & \sigma_{p_yp_y} \end{pmatrix}, \tag{3}$$

whose elements, $\sigma_{\alpha\beta}$, are the sample covariances between phase-space dimensions.

The measured transverse normalised emittance is represented for each momentum bin in figure 6. The horizontal error bars represent the limits of each momentum slice while the vertical error bars are purely statistical errors on the measurements. Systematic error studies are under way but preliminary results indicate that that they are small in comparison. The binned emittances are consistent across the range of studied momenta. The mean measured transverse normalised emittance for the whole sample is $3.85 \pm 0.04\,\mathrm{mm}$.

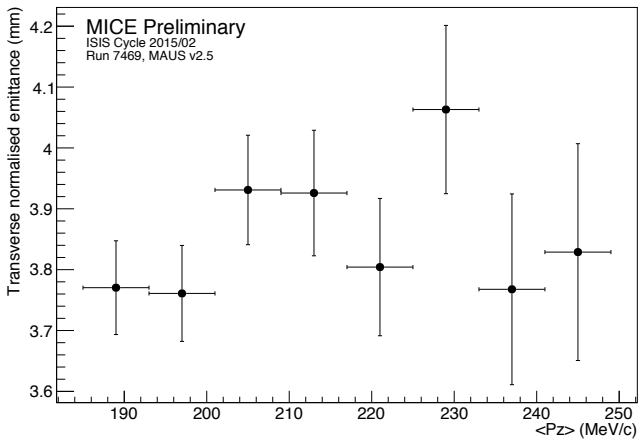

Figure 6 – Transverse normalised emittance of $8\,\mathrm{MeV}/c$ longitudinal momentum bins.

6 Recent update and short term prospects

The two spectrometer solenoids were powered together with the focus coil for the first time in July 2016. The beam was sampled up and downstream of the absorber focus coil module with the two trackers in a symmetrical fashion.

Analyses of the data are in progress. Figure 7 shows the reconstructed space point up and downstream in every station of both trackers. The stations are ordered from 5 to 1 before the absorber and from 1 to 5 after so that station 1 is always closest to the absorber.

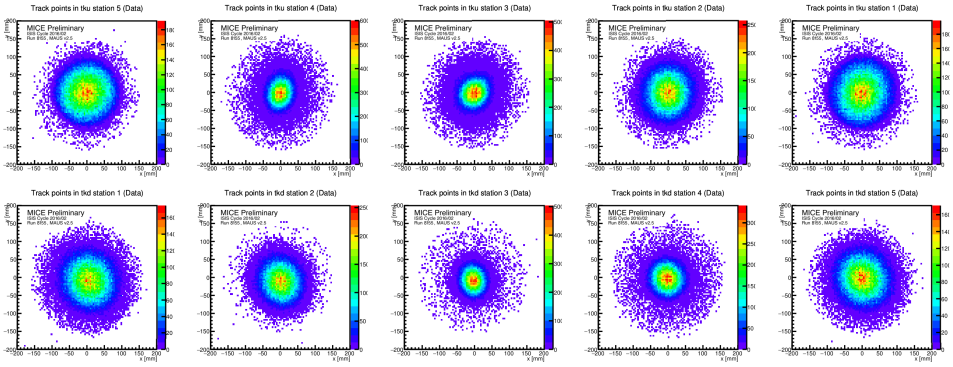

Figure 7 – Space point distributions in both trackers. The stations are ordered from the most upstream to the most downstream, i.e. from 5 to 1 upstream and from 1 to 5 downstream.

In the short-term, all the cooling channel superconducting magnets will be powered in different lattice configurations to allow for the measurement of transverse normalised emittance reduction at selected input emittances and momenta. A genetic algorithm was used to optimize the magnetic lattice for increased phase-space volume reduction and transmission for each considered input beam [11].

Significant transverse normalised emittance reduction is expected to be measured. A typical case would include a 200 MeV/c mean momentum and a 6 mm input emittance setting. The optimal magnetic lattice involves the magnets configured in "flip" mode, i.e. with the downstream coils in the opposite polarity to the ones upstream, as this configuration provides a tighter focus at the absorber. Figure 8 shows the simulated evolution of the transverse normalised emittance in the MICE Step IV cooling channel for this particular setting and a 65 mm-thick lithium hydride absorber. The rebound downstream of the absorber is due to filamentation and can be dealt with using a more advanced phase-space volume calculation. The simulated reduction going through the absorber is $\sim 4.8\,\%$ and $\sim 2.7\,\%$ when comparing the downstream to the upstream reference plane. The simulation ran on a sample of 10000 muons and yielded a transmission of 98.08 %.

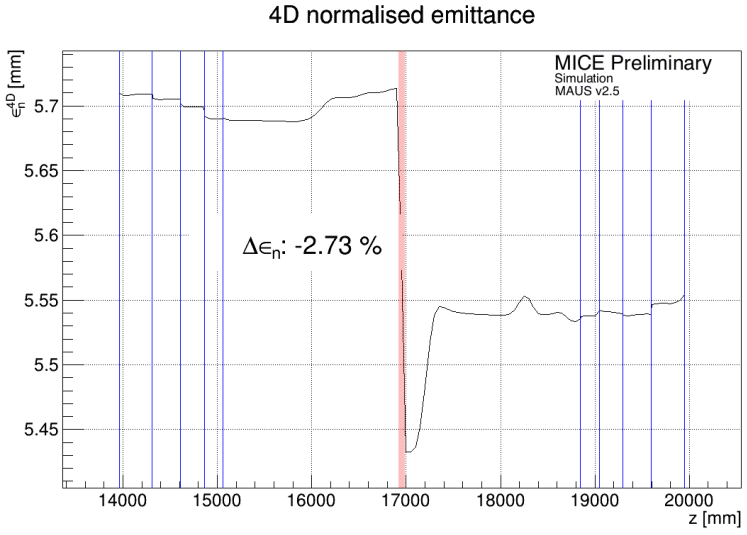

Figure 8 – Evolution of the transverse normalised emittance in the MICE Step IV cooling channel for the 6 mm–200 MeV/c beam in the "flip" mode lattice configuration. The red band shows the position and thickness of the absorber. Blue lines are places at the locations of the ten tracker stations.

7 Conclusions

MICE reached a milestone when the upstream scintillating-fibre tracker was immersed in a nominal uniform 4 T field for the first time during the commissioning of the spectrometer solenoid in October 2015. The data sample recorded during this period allowed for the phase-space volume of the muon beam to be measured on a particle-by-particle basis using the MICE tracker. The transverse normalised emittance was calculated for eight 8 MeV/c momentum bins for an average of 3.85 ± 0.04 mm and showed no significant variation across the momentum range.

Acknowledgments

The work described here was made possible by grants from Department of Energy and National Science Foundation (U.S.A.), the Instituto Nazionale di Fisica Nucleare (Italy), the Science and Technology Facilities Council (U.K.), the European Community under the European Commission Framework Programme 7 (AIDA project, grant agreement no. 262025, TIARA project, grant agreement no. 261905, and EuCARD), the Japan Society for the Promotion of Science and the Swiss National Science Foundation, in the framework of the SCOPES programme. We gratefully acknowledge all sources of support.

We are also grateful to the staff of the ISIS Department at the Rutherford Appleton Laboratory for the reliable operation of ISIS. We acknowledge the use of Grid computing resources deployed and operated by GridPP in the U.K., http://www.gridpp.ac.uk/.

References

1. M. Apollonio *et al, Nuc. Phys. Proc. Suppl.* 229–232, 515 (2012)
2. M. Alsharoa *et al, Phys. Rev. ST Accel. Beams* 6, 081001 (2003).
3. V. Parkhomchuck and A. Skrinsky, *Rev. Accel. Sci. Tech.* 1 no. 1, 237 (2008).
4. D. Stratakis and R. Palmer, *Phys. Rev. ST Accel. Beams* 18, 031003 (2015)
5. M. Yoshida *et al, Nuc. Phys. Proc. Suppl.* 149, 94–98 (2005)
6. C. N. Booth *et al, JINST* 8, P03006 (2013)
7. D. Adams *et al, JINST* 10, P12012 (2015)
8. M. Ellis *et al., NIM* **A** 659, 136–153 (2011)
9. D. Adams *et al, JINST* 11, P03001 (2016)
10. A. Dobbs *et al, J. Phys.: Conf. Ser.* 513, 022008 (2014)
11. A. Liu *et al, JACoW* 7, IPAC-2016-TUPMY006, 1553–1555 (2016)